Extended Base Speed Range by Using a Current-Source-Inverter-Fed IPMSM for Automotive Application

S. von Malottki*,**, K. Hameyer**
* DAIMLER AG
HPC G252, 70546
Stuttgart, Germany
Tel.: +49 / 7111734451
E-Mail: sicong.von_malottki@daimler.com
URL: http://www.daimler.com
** Institute of Electrical Machines (IEM), RWTH Aachen University
Schinkelstraße 4, 52062
Aachen, Germany
Tel.: +49 / 241 80 97667
E-Mail: post@iem.rwth-aachen.de
URL: http://www.iem.rwth-aachen.com

Keywords

Current Source Inverter (CSI), Automotive Application, Electric vehicle, Converter machine interactions, Power converters for EV

Abstract

This paper proposes a power train structure including a CSI with an integrated buck-converter to feed an IPMSM for automotive application. An optimized operation strategy to 1) extend the base speed range and 2) maximize the system efficiency is introduced. Simulated system performance and efficiency are presented and compared to the conventional VSI-based power train.

Introduction

Depending on the dc-link energy storage components, inverter topologies can be basically grouped into two main categories: voltage-source and current-source topologies [2]. While the VSIs use dc capacitors in the dc-link circuits, the current-source-inverters (CSIs) employ dc inductors in the dc-link circuits. For all Battery Electric Vehicles (BEVs) existing on the market so far a voltage source inverter (VSI) is exclusively used as the DC/AC converter. The widespread electrical machine is the Interior Permanent Magnet Synchronous Motor (IPMSM) because of its high starting torque and its wide constant-power speed area, due to the high energy content of rare earth materials such as neodymium-iron-born (Nd-Fe-B) and samarium-colbalt (Sm-Co) [1]. In the past years research works on using a CSI for electric vehicles have been investigated in [2], [3], [8], [9]. A CSI transferring the electrical variables voltage and current within electrical power train for automotive applications is gaining interests.

This paper proposes a system consideration of using a CSI with an integrated buck-converter as DC/AC-converter. The functionality of the converter components is explained in Section III. The advantage of using a CSI to extend the base speed range is described in Section IV. A developed operation strategy to feed an IPMSM is investigated with the intention of minimizing the semiconductor losses is explained as well. Section V presents simulated results of the system performance and efficiency of the proposed converter structure. A comparison to VSI feeding an IPMSM (as the current available technology) is conducted as well.

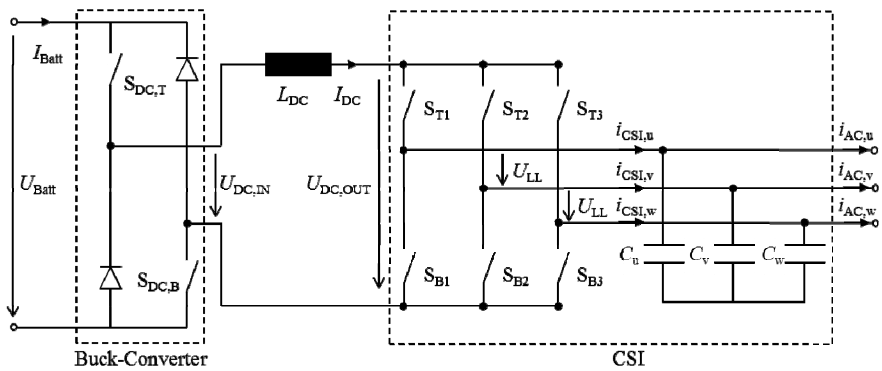

Fig. 1: Proposed structure of CSI with an integrated Buck-Converter for automotive application.

CSI with a buck-converter and its functionality

The proposed structure of CSI with an integrated buck- converter for automotive application is shown in Fig. 1. The semiconductor devices of CSI include 6 active switches and three filter capacitors for each phase at the output of the inverter. Since the CSI is considered being operated with constant dc link current, the switching devices must provide positive as well as negative blocking voltage.

According to the current state of technology, IGBTs with reverse-blocking characteristic are rarely available. That is why in case of CSI it is necessary to connect a diode in series instead of anti-parallel in comparison to a VSI. With the filter capacitor at the output of the CSI sinusoidal phase currents as well as voltages can be provided while feeding the IPMSM.

State	S_{T1}	S_{B1}	S_{T2}	S_{B2}	S_{T3}	S_{B3}	$I_{CSI,[a\ b\ c]}$
1	1	0	0	0	0	1	$[I_{DC}\ 0\ -I_{DC}]$
2	1	0		1	0		$[I_{DC}\ -I_{DC}\ 0]$
3	0	0	0	1	1	0	$[0\ -I_{DC}\ I_{DC}]$
4	0	1	0	0	1	0	$[-I_{DC}\ 0\ I_{DC}]$
5	0	1	1	0	0	0	$[-I_{DC}\ I_{DC}\ 0]$
6	0	0	1	0	0	1	$[0\ I_{DC}\ -I_{DC}]$
7	1	1	0	0	0	0	[0 0 0]
8	0	0	1	1	0	0	[0 0 0]
9	0	0	0	0	1	1	[0 0 0]

Tab. 1: Switching states of a CSI and its output currents.

State CSI S_{T1}-S_{B3}	buck-converter $[S_{DC,T}\ S_{DC,B}]$	$U_{DC,IN}$	$U_{DC,OUT}$
State 7-9	[1 1]	U_{Batt}	0
	[0 0]	$-U_{Batt}$	0
	[0 1]/[1 0]	0	0
State 1-6	[1 1]	U_{Batt}	U_{LL}
	[0 0]	$-U_{Batt}$	U_{LL}
	[0 1]/[1 0]	0	U_{LL}

Tab. 2: Switching states of the buck-converter and its output voltages.

An asymmetrical half bridge is used as a buck-converter as a DC/DC-converter. Its necessity is explained with the following three reasons: 1) Because of the fact that the dc link current of the CSI must be positive, it is only possible to provide the generator mode to charge the battery during recuperation by reversing the polarity of the input voltage of the CSI. This can be done with the provided buck-boost-converter. 2) A decoupling between the battery current level and the dc link current level is achieved by using the buck-converter. This way the semiconductor losses are able to be minimized by the operation strategy. 3) While a VSI operating as a buck-converter, a CSI has the advantage of boosting its output voltages. This function is detailed described in [2]. This is the main reason why the base speed range can be extended by using a CSI. However in order to take this advantage, the dc link current must be increased. This will be detailed explained in Section IV. The buck-converter is integrated to fulfill this aim.

Generally the basic principle of Pulse-Width-Modulation (PWM) can be implemented to control CSI. In differ to VSI where two or three switches must be turned on during one PWM period, only two switches, each one of the top and button side of the inverter are turned on at the same time. While two zero states for VSI exist by turning on all three top or all three button switches of the inverter [3], the zero states for CSI are conducted by turning on both the top and button switches of one phase to induce a short circuit [4], [5]. This way the dc link current is increased. Tab.1. presents the switching states of a CSI and its output currents.

Depending on the switching states of the buck-converter the input voltage of the CSI $U_{DC,OUT}$ becomes the positive or the negative voltage of the energy storage, hence the recuperation mode to charge the battery is possible with a constant positive dc link current. Tab. 2 presents the switching states of the buck-converter and its output voltages.

Proposed operation strategy

As mentioned in Section III the flexibility of decoupling the current level from the battery current and the dc link current is given by the integration of the buck-converter. Details of the control strategy of CSI are explained in [2]. A stable dc link current is one requirement concerning the control of CSI. In [4] the harmonic performance of the phase currents affected by the level of the dc link current is discussed. Due to the fact that the top and button switches of the CSI must be turned on at the same time during one PWM period, the entire dc link current flows through the CSI. This leads to two effects: 1) the conduction losses of the semiconductor devices are directly proportional the level of the dc link current. 2) the minimal level of the dc link current must be equal to the peak values of the phase current to achieve sinusoidal performance.

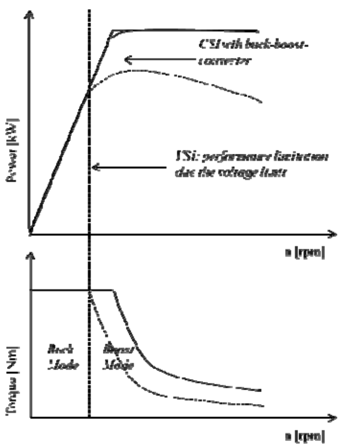

Fig. 2: Buck and boost mode while operating with CSI with extended base speed range.

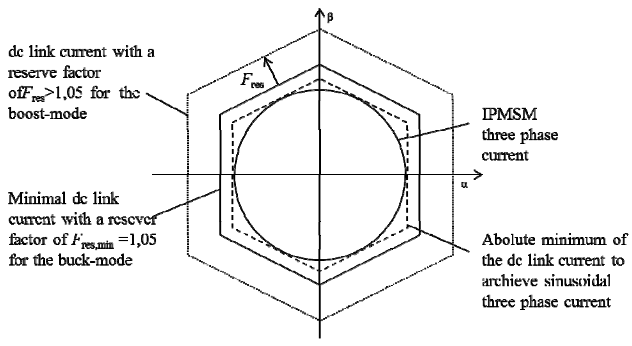

Fig. 3: dc link current level for the proposed operation strategy in order to reduce the losses in CSI and feed the IPMSM for the boost and buck mode.

Based on the above consideration the trade-off criterions to define the level of the dc link current can be summarized as following:

- The higher the dc link current is chosen, the better the harmonic performance of the three phase currents become.
- The higher the dc link current is chosen, the lower the system efficiency becomes.

For the following consideration the entire operation range of the IPMSM is devised into two modes: the buck-and the boost mode, as shown in Fig. 2.

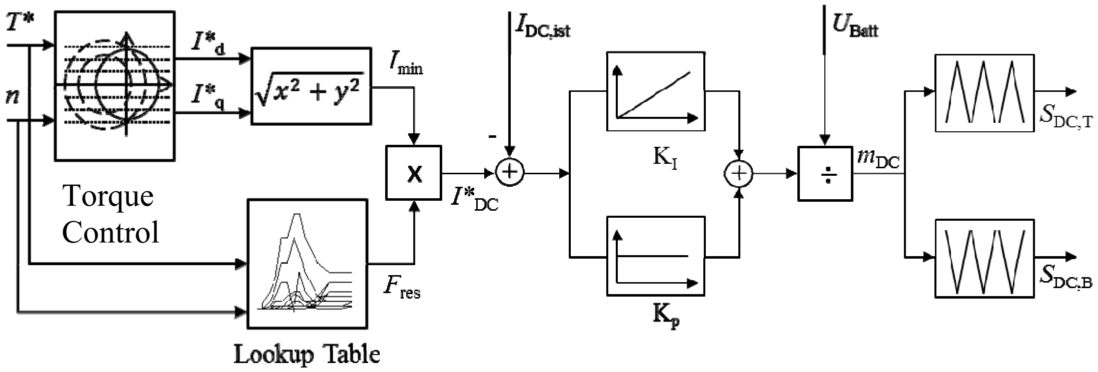

Fig. 4: Control structure of the proposed operation strategy.

Buck Mode

The buck mode can be described as the base speed mode. In this operation area the level of the line-to-line voltages of IPMSM is below the level of the battery voltage. In this case level of the dc link current must be covered by the peak value of the three phase current of the IPMSM. According to the torque requirement the reference values for the three phases are given as the current components I_d and I_q [1]. In order to achieve good harmonic performance of the three phase current a reserve factor of $F_{res} = 1.05$ is used to multiple with the peak value calculated by I_d and I_q.

Boost Mode

The boost mode begins with the field weakening area according to the classic definition. In this area the line-to-line voltage of the IPMSM becomes higher than the battery voltage. By using a VSI as DC/AC-converter the IPMSM must be fed with the current component I_d in order to reduce the magnetic field and therefore to be supplied with the correct amount of current to fulfill the torque requirement. Due to the possibility of CSI boosting the output voltages, it is not necessary to reduce the magnetic field. While leading in the zero states (s. Tab. 1) a short circuit is created to increase the dc link current. The output voltage is then boosted with the energy stored during the zero states. In this case the reserve factor must be higher to increase the reference value of the dc link current. The reserve factor for the boost mode can be calculated as shown in Tab. 3.

$$m_{DC} = \frac{\bar{U}_{DC,IN}}{U_{Batt}} = \frac{I_{Batt}}{I_{DC}} \quad (1) \qquad m_{CSI} = \frac{\bar{U}_{DC,OUT}}{\sqrt{3} \cdot u_{LL}} \quad (2) \qquad m_{ges} = \frac{u_{LL}}{U_{Batt}} = \frac{m_{DC}}{\sqrt{3} \cdot m_{CSI}} \quad (3)$$

By varying the reserve factor F_{res} the dc link current is only increase in the operation range when the boost function of the CSI is needed. This way the dc link current is minimized for each working point. The level of the dc link current is explained with Fig. 3. Hence, the relations between the input and output voltages from the DC and AC side of the power train is influenced by the reserve factor as well. (1) – (3) present the relations between the voltages through the modulation indexes m_{DC} and m_{CSI}, which are used each to control the buck- converter and the CSI. While the control strategy of CSI is detailed in [2], the control structure of the buck-converter is shown in Fig. 4. In Tab. 3 the relevant values each for the buck and boost mode are presented in Tab. 3.

	m_{DC}	$\hat{m}_{CSI}$	F_{res}	I_{DC}^*	m_{ges}
Buck Mode: $\frac{\hat{u}_{LL}}{u_{Batt}} \leq \frac{2}{\sqrt{3}}$	$\frac{I_{Batt}}{I_{DC}}$	0,95	1.05	$\sqrt{I_d^2 + I_q^2} \cdot 1.05$	$\frac{2}{\sqrt{3}} \cdot 1.05 \cdot m_{DC}$
Boost Mode: $\frac{\hat{u}_{LL}}{u_{Batt}} > \frac{2}{\sqrt{3}}$	0.95	$\frac{1}{F_{res}}$	$\frac{I_{Batt}}{\sqrt{I_d^2 + I_q^2} \cdot 0.95}$	$\sqrt{I_d^2 + I_q^2} \cdot F_{res}$	$\frac{2}{\sqrt{3}} \cdot F_{res} \cdot 0.95$

Tab. 3: Relevant relations for operating the IPMSM eath for the buck and boost mode.

Simulation results

Simulation model

The control structure of the proposed operation strategy in Fig. 4 and the torque control for an IPMSM presented in [2] are implemented in MATLAB/Simulink environment. The electrical system components are built in Plecs Blockset. The model of the IPMSM is implemented with Look Up Tables (LUT) of its FEM-calculated inductances in d- q- axis and its permanent magnet flux. Losses of the IPMSM is calculated with a FEM simulation and integrated into the loss calculation of the system. The structure of the model is illustrated in Fig. 5.

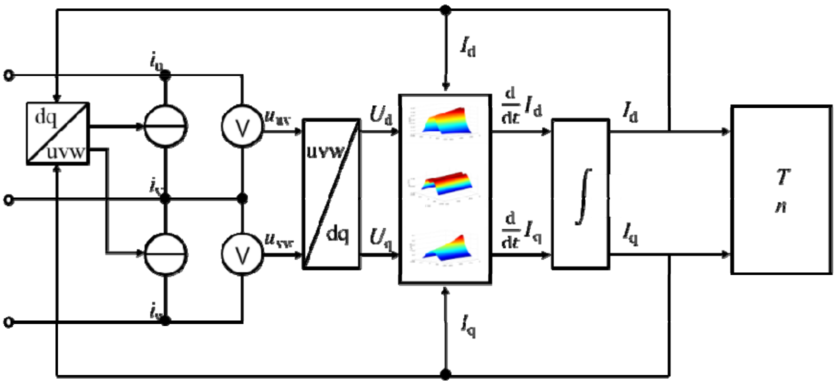

Fig. 5: Structure of the IPMSM model with implemented LUT of its FEM-calculated inductances in d- and q-axis and permanent magnet flux.

A thermal model of the proposed DC/AC-converter structure of the CSI and the buck-converter is built with the method explained in [7] (Fig. 6). The semiconductor losses of the chosen power electronic modules are integrated into the thermal model as LUT. With the built simulation model steady-state working point as well as dynamic performances can be simulated.

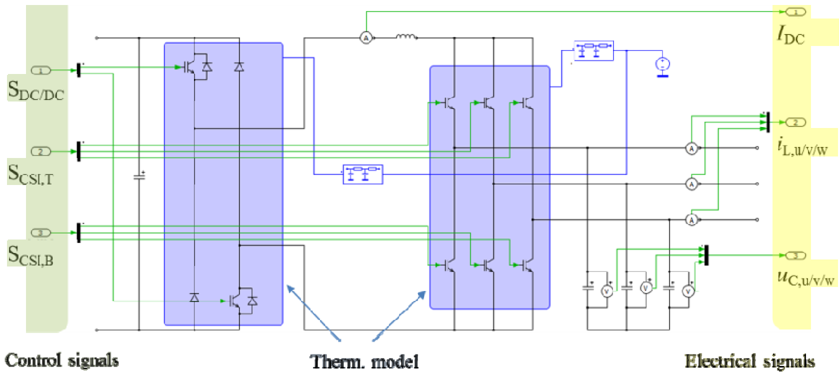

Fig. 6: Thermal model of the proposed DC/AC-converter structure of the CSI and the buck-converter.

Dynamic Performance

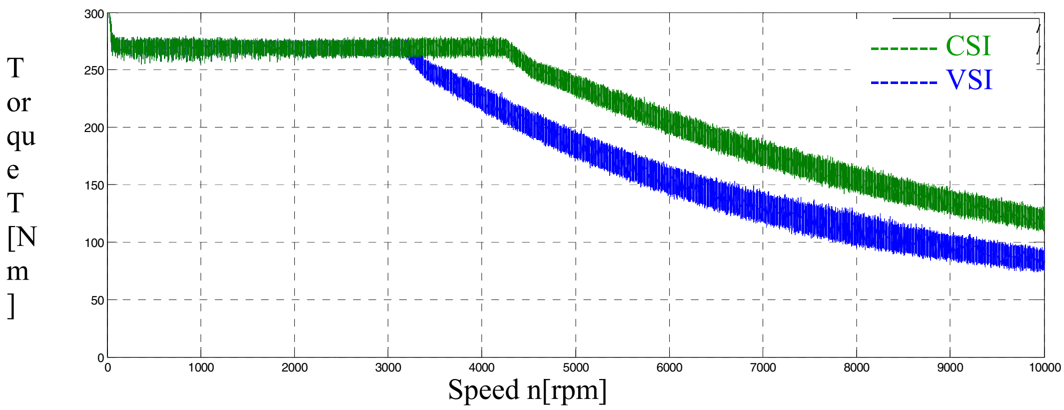

Fig. 7: Dynamic speeding-up of the simulated IPMSM @ full load power with U_{batt} = 300 V.

Under the condition of a battery voltage of 300 V the same IPMSM is fed with a VSI and the proposed converter structure in this paper (Fig. 1.) The optimum control strategy for IPMSM in constant torque and flux weakening range presented in [1] is implemented for both converter structures.

While using a field oriented control and the standard sinusoidal PWM for VSI the base speed range ends when the battery voltage limit is reached, the base speed range is extended by using the operation strategy with the presented control structure in Fig. 7 with CSI. The performance of the IPMSM is not limited by the battery voltage, but by the reverse blocking voltage of the chosen IGBTs with 650 V. Using IGBTs with reverse blocking voltages of 1200 V, the base speed range can be extended to an even higher speed.

System Efficiency

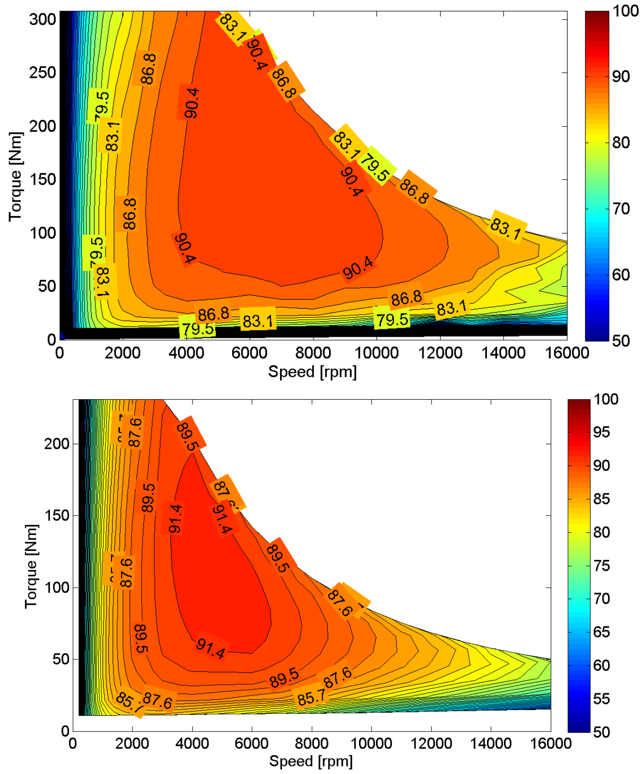

Fig. 8: System efficiency of the IPMSM with the proposed DC/AC-converter including CSI and a buck-converter (r.) and a VSI (l.) @ U_{batt}=300V.

System efficiency of the power train system components consisting of IPMSM and the converter are presented in Fig. 8. The IPMSM is fed with a VSI and the proposed converter structure presented in this paper (Fig. 1). The calculated losses include 1) power electronic conduction and switching losses of each semiconductor device 2) iron losses of the IPMSM from FEM calculation 3) friction losses from measurement.

It is obvious that CSI with the integrated buck-converter as presented in this paper cause more losses. The higher power electronic losses can be explained, on the one hand by the amount of semiconductor components used in the structure in comparison to the components of a VSI, on the other hand as explained in Section IV, the conduction losses of the semiconductor devices are influenced by the dc link current by using CSI. Since an IPMSM is taken as the traction machine, which is originally designed and optimized for being fed by a VSI, the machine is fed with a high current component I_d over the entire operation range in order to archive high torque density. Therefore a high dc link current is needed in the entire operation range. Nevertheless by using the operation strategy presented in Section IV, the dc link current can be kept as low as possible which is intent to minimize the converter losses.

Considering the integration of a CSI fed electrical machine in to the power train for automotive application, the machine design for CSI must be reconsidered. A purpose design to emphasize the advantage of the CSI in order to optimize the system efficiency will be investigated in future research work.

Conclusion

This paper deals with a system consideration of using a CSI-fed IPMSM for automotive application. The proposed converter structure includes a CSI with an integrated buck-converter. The functionality of the components and their advantages for the system performance are explained. The disadvantage concerning system efficiency is pointed out. A developed operation strategy to feed an IPMSM in order to minimize the semiconductor losses is presented. Simulated results of the system performance and efficiency are presented in this paper. A comparison between VSI according to state of technology and the proposed converter structure is conducted.

References

[1] M. Meyer, J. Boecker, "Optimum Control for Interior Permanent Magnet Synchronous Motors (IPMSM) in Constant Torque and Flux Weakeing Range", Power Electronics and Motion Control Conference, 2006.

[2] S. Liu, K. Hameyer, "A Current Source Inverter for Battery Electric Vehicles", 15th European Conference on Power Electronics and Applications, 2013.

[3] A. Ackva, "Spannungseinprägendes Antriebssystem mit Synchronmachine und direkter Stromregelung, Verlag der Augustinus-Buchhandlung", Aachen, 1992.

[4] A. Kloenne, "Regelungs- und Modulationsstrategien für den Stromzwischenkreisumrichter mit Asynchronmaschine", Shaker Verlag, 2003.

[5] M. Bierhoff, "Ein Vergleich von Netzpulsstromrichtern mit eingeprägtem Gleichstrom und eingeprägter Gleichspannung im Zwischenkreis", Shaker Verlag, 2008.

[6] R. De Doncker, D. W.J. Pulle, A. Veltman "Advanced Electric Drives", Springer, 2011

[7] J. Schönberger, "Averaging Methods for Electrical-Thermal Converter Models, 14th European Conference on Power Electronics and Application, 2011.

[8] G. Su, L. Tang, Z. Wu, "Extended Constant-Torque and Constant-Power Speed Range Control of Permanent Magnet Machine Using a Current Source Inverter", Vehicle Power and Propulsion Conference, 2009.

[9] G. Su, L.Tang, "Boost Mode Test of a Current-Source-Inverter-Fed Permanent Magnet Synchonous Motor Drive for Automotive Applications", Control and Modelling for Power Electronics, 2010.